Korean J. Chem. Eng., **24**(5), 888-891 (2007)

Structure and electrochemical characterization of $LiNi_{0.3}Co_{0.3}Mn_{0.3}Fe_{0.1}O_2$ cathode for lithium secondary battery

Jong-Tae Son† and Elton Cairns

Environmental Energy Technologies Division, E.O. Lawrence Berkeley National Laboratory, Berkeley, CA 94720, USA
(*Received 3 January 2007 • accepted 30 January 2007*)

Abstract−A lithium insertion material having the composition $LiNi_{0.3}Co_{0.3}Mn_{0.3}Fe_{0.1}O_2$ was synthesized by simple sol-gel method. The structural and electrochemical properties of the sample were investigated using X-ray diffraction spectroscopy (XRD) and the galvanostatic charge-discharge method. Rietvelt analysis of the XRD patterns shows that this compound can be classified as α-$NaFeO_2$ structure type (R3m; a=2.8689(5) Å and 14.296(5) Å in hexagonal setting). Rietvelt fitting shows that a relatively large amount of Fe and Ni ion occupy the Li layer (3a site) and a relatively large amount of Li occupies the transition metal layer (3b site). $LiNi_{0.3}Co_{0.3}Mn_{0.3}Fe_{0.1}O_2$ when cycled in the voltage range 4.3-2.8 V gives an initial discharge capacity of 120 mAh/g, and stable cycling performance. $LiNi_{0.3}Co_{0.3}Mn_{0.3}Fe_{0.1}O_2$ in the voltage range 2.8-4.5 V has a discharge capacity of 140 mAh/g, and exhibits a significant loss in capacity during cycling. Ex-situ XRD measurements were performed to study the structure changes of the samples after cycling between 2.8-4.3 V and 2.8-4.5 V for 20 cycles. The XRD and electrochemical results suggested that cation mixing in this layered structure oxide could be causing degradation of the cell capacity.

Key words: Cathode Material, $LiNi_{0.3}Co_{0.3}Mn_{0.3}Fe_{0.1}O_2$, Sol-gel, Lithium Ion Battery

INTRODUCTION

$LiCoO_2$, which is currently used as a cathode material for Li ion batteries, is easy to prepare and has good rechargeability even at high rates. However, due to its high cost and toxicity, an intensive search for new cathode materials has been underway. $LiNiO_2$ and have been extensively studied as possible alternatives to $LiCoO_2$. However, $LiNiO_2$ and $LiMnO_2$ have critical problems for practical applications. $LiNiO_2$ has received great interest as an alternative material due to its higher capacity of more than 170 mAh/g (In case of $LiCoO_2$: 150 mAh/g) with a high, smooth, and monotonic voltage profile [1-3]. However, this material could not be used due to difficulties in the synthesis of stoichiometric $LiNiO_2$ and instability of Ni^{4+} ions at high voltages, which resulted in a transformation into the NiO_2 phase at the surface of the particles during electrochemical cycling [4]. $LiMnO_2$ is not thermodynamically stable as the layered structure, but as an orthorhombic phase *o*-$LiMnO_2$ [5,6]. $LiMnO_2$ was observed to undergo a detrimental phase transformation to a defective spinel-related form through a minor atomic rearrangement during the first charge and subsequent cycling of Li, leading to the eventual degradation of electrode performance [7,8].

The combination of Mn, Co, and Ni as $LiNi_{1/3}Co_{1/3}Mn_{1/3}O_2$ was adopted by Ohzuku and Makimura to overcome the disadvantage of $LiNiO_2$ and $LiMnO_2$ [9-12]. $LiNi_{1/3}Co_{1/3}Mn_{1/3}O_2$ has the α-$NaFeO_2$ structure with space group R3m, which is characteristic of the layered $LiNiO_2$ and $LiMnO_2$ structure and showed the capacity of more than 170 mAh/g in the voltage range of 2.5-4.3 V with excellent cyclability and no transformation to the spinel phase during electrochemical cycling

Recently, Ceder et al. reported on $LiNi_{1/3}Fe_{1/6}Co_{1/6}Mn_{1/3}O_2$ as a new cathode material [13]. They claimed that Fe could be an advantageous doping material because Fe will lower the cell voltage during charge. Ceder et al. [13] also simulated a charge curve by using a first principles method [14]. Ceder et al. synthesized the $LiNi_{1/3}Fe_{1/6}Co_{1/6}Mn_{1/3}O_2$ compound at 750 °C by using a sol-gel method and it delivered an initial discharge capacity of 150 mAh/g at 2.8-4.5 V. The discharge capacities at 2.8-4.5 V decrease with cycling and remained at 120 mAh/g after 30 cycles, which is 80% of the initial capacity [13].

In this work, a simple sol-gel method is used for preparing $LiNi_{0.3}Co_{0.3}Mn_{0.3}Fe_{0.1}O_2$ cathode material. The structure and electrochemical properties of the powder were investigated using X-ray diffraction (XRD), cyclic voltammetry (CV), and a galvanostatic charge-discharge method. We examined the amount of cation mixing for our sample through Rietvelt analysis.

EXPERIMENTAL EQUIPMENT AND PROCEDURES

In the present study, we have adapted a simple sol gel process to the synthesis of $LiNi_{0.3}Co_{0.3}Mn_{0.3}Fe_{0.1}O_2$ from manganese acetate tetra-hydrate [$Mn(CH_3COO)_2 \cdot 4H_2O$], nickel(II) acetate tetra-hydrate [$Ni(CH_3COO) \cdot 4H_2O$], cobalt acetate tetra-hydrate [$Co(CH_3COO)_2 \cdot 4H_2O$], iron nitrate hexa-hydrate [$FeNO_3 \cdot 6H_2O$] and Lithium acetate di-hydrate [$Li(CH_3COO)_2 \cdot 2H_2O$]. Stoichiometric amounts of Mn, Ni, Co, Li acetate and Fe nitrate were dissolved in distilled water and stirred continuously at 80 °C for 4 h until a transparent sol was obtained. To remove water, the sol was heated at 100 °C for 3 hrs. As the evaporation of water proceeded, the sol turned into a viscous transparent gel. The obtained gel was first heated at 500 °C for 5 h in air, and then it was calcined at 1,000 °C for 10 h in air to obtain $LiNi_{0.3}Co_{0.3}Mn_{0.3}Fe_{0.1}O_2$ powder.

X-ray diffraction patterns for the cathodes were obtained using a Siemens D-5000 diffractometer in the 2θ range from 10 to 70° with

†To whom correspondence should be addressed.
E-mail: jtson@kaist.ac.kr

Cu Kα radiation (λ=1.5406 Å). The data was refined by the Rietvelt method using the Powder-cell program. The peak shape was described by a Pseudo-Voigt function. The background level was defined by a polynomial function. The scale factor, the counter zero point, the peak asymmetry and the unit-cell dimensions were refined in addition to the atomic parameters. Lattice parameters were determined by whole pattern fitting. For ex-situ XRD analysis on the cycled electrode, the cells were dismantled and washed with diethyl carbonate (DEC) two times to ensure the removal of absorbed Li salt and dried in a vacuum oven at 70 °C for 12 h. The morphology of the obtained powder was observed with a scanning electron microscope (SEM). Jong-Tae: please insert make and model of the SEM.

To prepare the positive electrode, 72% $LiNi_{03}Co_{03}Mn_{03}Fe_{0.1}O_2$, 10% SFG6 graphite, 10% acetylene black, N-methyl-2-pyrrolidinone and 8% PVdF (Kureha KF100) binder were mixed in a crucible. After two hours of grinding, the viscous slurry was coated on an aluminum foil using a doctor blade and a film of uniform thickness was obtained. The film was then dried at 60 °C for 6 h and 120 °C for 6 h in a vacuum oven. The thickness of the cathode film was about 40 μm. The Swagelok cell was assembled in a glove box using the above cathode film, lithium foil, porous polyethylene film (Celgard 2300) and 1.2 M $LiPF_6$ solution in 1 : 1 : 3 volume ratio of ethylene carbonate (EC)/propylene carbonate (PC)/dimethyl carbonate (DMC). Lithium metal foil was used as both the counter and reference electrode. After Swagelok cell assembly, the test cells were charged to 4.3 or 4.5 V versus Li/Li^+ with a current density of 0.1C (170 mA g^{-1} was assumed to be 1C rate) and then discharged to 2.8 V at the same current density.

RESULTS AND DISCUSSION

1. Powder Characterization

Rietvelt analysis has been performed to understand the structural properties of the sample. Cation mixing in the layered oxides can deteriorate cell performance [15,16]. Therefore, we examined the amount of cation mixing through Rietvelt fitting. It is assumed that Li, Fe and Ni are on the 3a sites, Ni, Co, Mn, Fe and Li are on the 3b sites, and oxygen is on the 6c sites. Since the radius of the Fe^{3+} (0.69 Å) and Ni^{2+} cation (0.69 Å) are close to that of Li^+ (0.76 Å) [13], it is considered that Ni, Fe and Li atoms may exchange between 3a and 3b sites and that the stoichiometry of the powders is fixed to the nominal values of the starting materials in the Rietvelt fitting.

The XRD pattern of $LiNi_{03}Co_{03}Mn_{03}Fe_{0.1}O_2$ is presented in Fig. 1a together with its calculated pattern based on the Rietvelt fit. The sample can be fitted well with the α-$NaFeO_2$ structure (space group: R-3m, 166). This result indicates that layered $LiNi_{03}Co_{03}Mn_{03}Fe_{0.1}O_2$ was successfully synthesized by a simple sol-gel method. The unit cell parameters for the hexagonal cell are a=2.8689 Å and c=14.2962 Å, and the c/a ratio is 4.976. This c/a ratio is nearly the same as that of $LiCoO_2$ (4.99) [17]. The best Rietvelt refinement results for the sample are listed in Table 1. The percentages of site occupation for 3a sites (0 0 0) by Li, Ni and Fe ions are 89.8, 4.9 and 5.3%, respectively. It is certain that a larger amount of iron occupies 3a sites (5.3%) compared to the 3b sites (4.3%). In addition, the observed diffraction lines show a small integrated peak ratio (0 0 3) to (1 0 4) of 0.97 which suggests some cation disorder in the host structure [18]. Thus, we had expected that $LiNi_{03}Co_{03}Mn_{03}Fe_{01}O_2$ might show better electrochemical properties when cycled in a low cut-off voltage region (a smaller amount of Li will be inserted and extracted in this region). The morphology of the powder was observed with a scanning electron microscope (SEM) as shown in Fig. 2. Some

Table 1. Rietvelt refinement results for $LiNi_{0.3}Co_{0.3}Mn_{0.3}Fe_0O_2$

Lattice parameter				
a (Å)=2.8710±0.0004	c (Å)=14.2874±0.0006	R (c/a) = 4.9765		
Site occupation on 3a site				
Li=0.898	Ni=0.049	Fe=0.053		
Site occupation on 3b site				
Li=0.082	Ni=0.287	Mn=0.294	Co=0.293	Fe=0.043
R_p (%)=13.2	R_{wp} (%)=18.2	R_B (%)=4.5		

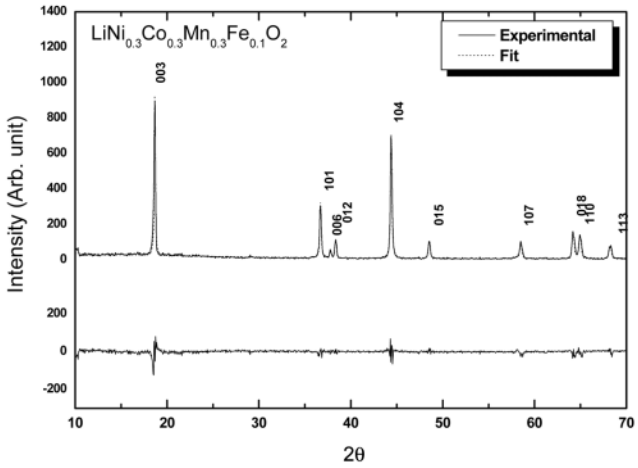

Fig. 1. Experimental XRD patterns and calculated patterns from Rietvelt program for $LiNi_{0.3}Co_{0.3}Mn_{0.3}Fe_{0.1}O_2$ compound. Difference between data and calculation is given in lower panel.

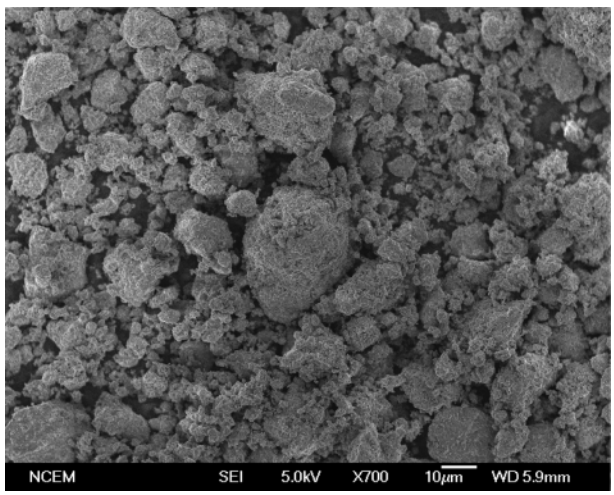

Fig. 2. SEM image of $LiNi_{0.3}Co_{0.3}Mn_{0.3}Fe_{0.1}O_2$ compound prepared by simple sol-gel method calcined at 1,000 °C for 10 h.

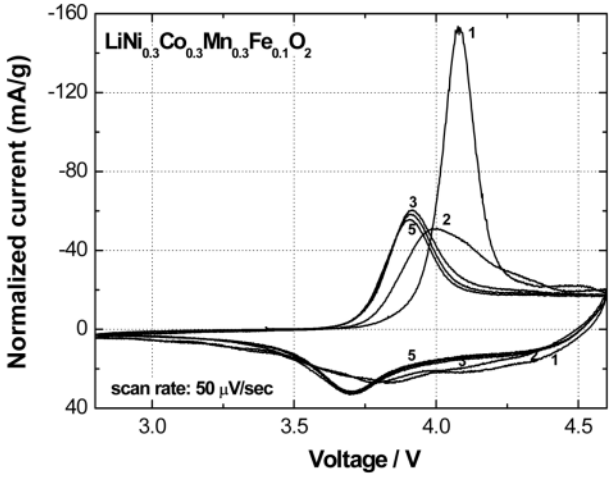

Fig. 3. Cyclic voltammertry of the $LiNi_{0.3}Co_{0.3}Mn_{0.3}Fe_{0.1}O_2$ cell between 2.8 and 4.6 V at a scan rate of 50 μV s^{-1}.

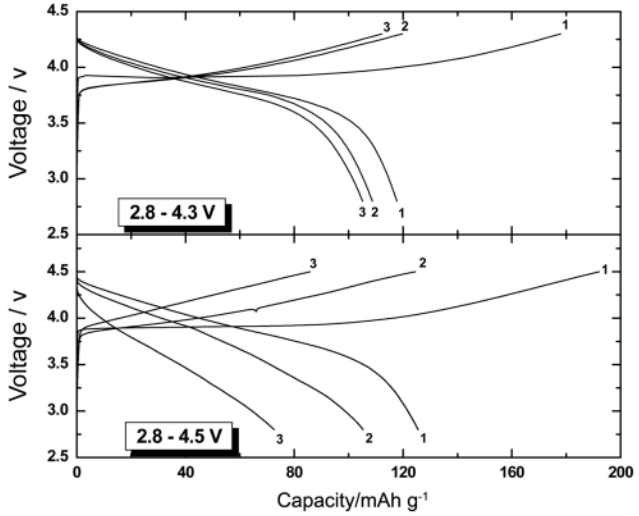

Fig. 4. First three charge-discharge curves for the $LiNi_{0.3}Co_{0.3}Mn_{0.3}Fe_0O_2$ sample cycled in various voltage ranges at a constant current density of 17 mA/g.

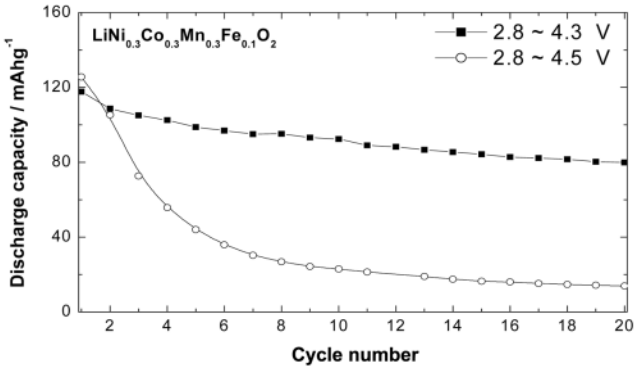

Fig. 5. Cycle performance of $LiNi_{0.3}Co_{0.3}Mn_{0.3}Fe_0O_2$ compound in various voltage ranges at a constant current density of 17 mA/g.

regions show severe segregation of particles.

2. Electrochemical Behavior

The cyclic voltammetry (CV) of the $LiNi_{0.3}Co_{0.3}Mn_{0.3}Fe_{0.1}O_2$ cell for the first five cycles is shown in Fig. 3. The important feature is the difference between the first and subsequent cycles. The first anodic scan has two oxidation peaks, a major sharp peak centered at 4.07 V and a minor broad one at 4.5 V, and a small broad cathodic peak centered at 3.82 V. It can be seen that the peak at 4.07 V in the first anodic scan was shifted by 0.07 V to lower voltage on the second anodic scan and significantly decreased in intensity and area after the first cycle. However, the 3.82 V peak in the first cathodic scan was slightly shifted by 0.02 V to lower voltage and had a similar intensity and area during the second cycle. On subsequent cycles, the oxidation and reduction processes show only one major peak centered at 4.0 V and 3.8 V, respectively. The difference of shape and area for the anodic and cathodic peaks during the first cycle implies that structural changes are taking place during the first lithium extraction of $LiNi_{0.3}Co_{0.3}Mn_{0.3}Fe_{0.1}O_2$. As can be seen in Table 1, the $LiNi_{0.3}Co_{0.3}Mn_{0.3}Fe_{0.1}O_2$ cathode has a large amount of cation mixing in the 3a site (0 0 0). Therefore, if Li was extracted fully from the 3a sites, the structure of $LiNi_{0.3}Co_{0.3}Mn_{0.3}Fe_{0.1}O_2$ might be changed to another one that does not readily intercalate Li. To investigate this idea, we adopted the following strategy.

(1) Different amounts of Li extraction: Electrochemical cycling was performed on the cells between 2.8-4.3 V and 2.8-4.5 V for 20 cycles.

(2) Structural change observation after cycling: Ex-situ XRD measurements were performed to study the structural changes of the samples after cycling between 2.8-4.3 V and 2.8-4.5 V for 20 cycles.

The first three charge-discharge curves for the $LiNi_{0.3}Co_{0.3}Mn_{0.3}Fe_{0.1}O_2$ cell cycled in various voltage ranges at a constant specific current of 17 mA/g are shown in Fig. 4. The $LiNi_{0.3}Co_{0.3}Mn_{0.3}Fe_{0.1}O_2$ cell has a very smooth and monotonic voltage profile, similar to the voltage profiles of the $LiNi_{1/3}Co_{1/3}Mn_{1/3}O_2$ cell reported by other researchers [19,20]. The $LiNi_{0.3}Co_{0.3}Mn_{0.3}Fe_{0.1}O_2$ in the voltage range 2.8-4.5 V has an initial charge capacity of 126 mAh/g with an irreversible capacity loss of 67 mAh/g. On the other hand $LiNi_{0.3}Co_{0.3}Mn_{0.3}Fe_{0.1}O_2$ in the voltage range 2.8-4.3 V yields an initial capacity of 118 mAh/g with an irreversible capacity loss of 60 mAh/g. The IR drop during the first discharge is about 0.1 V when cycled between 2.8-4.5 V, and is about 0.025 V when cycled between 2.8-4.3 V.

The cycling performance of the cells with $LiNi_{0.3}Co_{0.3}Mn_{0.3}Fe_{0.1}O_2$ is shown in Fig. 5 as a function of cycle number for a cell operating at 0.1C (17 mA/g) rate when cycled between 2.8-4.3 and 2.8-4.5 V. The discharge capacities at 2.8-4.3 and 2.8-4.5 V decrease with cycling and remain at 80 and 14 mAh/g after 20 cycles, which are 68 and 11% of the initial capacities, respectively. Cycling results show that with decreasing cut-off voltage, the cell exhibited more stable cyclability.

To investigate the change of structure, we examined the XRD patterns after cycling. The XRD pattern of $LiNi_{0.3}Co_{0.3}Mn_{0.3}Fe_{0.1}O_2$ after 20 charge/discharge cycles at 0.1C (17 mAh/g) is presented in Fig. 6. We noticed two major differences between the cycled cathode and the as-prepared cathode. First, the (0 0 6) line disappears after cycling, as shown in Fig. 6. The disappearance of the (0 0 6) line is a very similar result to that of charged $LiNi_{0.3}Co_{0.3}Mn_{0.3}O_2$ [17]. It may indicate that a Li-poor cathode structure was formed

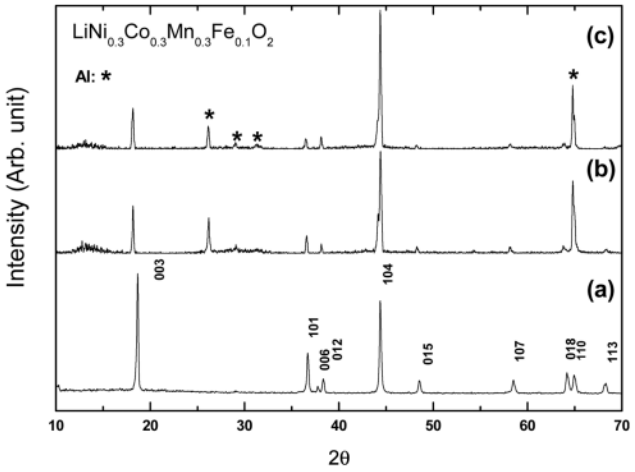

Fig. 6. X-ray diffraction patterns of: (a) $LiNi_{0.3}Co_{0.3}Mn_{0.3}Fe_{0.1}O_2$ as-prepared; (b) discharged electrode after 20 charge-discharge cycles (2.8-4.3 V); (c) discharged electrode after 20 charge-discharge cycles (2.8-4.5 V).

Table 2. Lattice parameters and the integrated intensity ratio of 003/104 lines before and after cycling

	a (Å)	c (Å)	c/a	$R_{003/104}$
As prepared	2.8689±0.0007	14.296±0.005	4.98	0.97
After 20 cycles (2.8-4.3 V)	2.860±0.003	14.33±0.03	5.01	0.26
After 20 cycles (2.8-4.5 V)	2.857±0.003	14.28±0.02	5.00	0.20

after charge-discharge cycling. Second, the integrated peak ratio (0 0 3) to (1 0 4) dramatically decreases after cycling. These results show that cation mixing is increased during cycling, especially when cycled over the range 2.8-4.5 V (large amount of Li will be inserted and extracted in this region) compared to the 2.8-4.3 V region. The integrated intensity ratio (R=0.21) is lower for the cell after 20 cycles in the range, 2.8-4.5 V as compared to that (R=0.26) for cycling between 2.8 and 4.3 V after 20 cycles. This indicates that the higher voltage cycling leads to an increased cation mixing. Therefore, we found that cation mixing has a very important role in the electrochemical cycling of $LiNi_{0.3}Co_{0.3}Mn_{0.3}Fe_{0.1}O_2$. Unit cell parameters and the ratio of the integrated peak ratio (0 0 3) to (1 0 4) are summarized in Table 2. The increased c/a values indicate that a larger number of (larger size) Li^+ ions are occupying the M site (increased cation mixing).

CONCLUSIONS

The layered material $LiNi_{0.3}Co_{0.3}Mn_{0.3}F_{0.1}O_2$ was synthesized by using a simple sol-gel method. The amount of ion mixing between Li, Fe and Ni was determined by Rietvelt refinement. The exchange of (Ni+Fe) with Li atoms is about 0.1 atom fraction, which is a large amount.

$LiNi_{0.3}Co_{0.3}Mn_{0.3}Fe_{0.1}O_2$ in the voltage range 2.8-4.5 V has an initial discharge capacity of 126 mAh/g with an irreversible capacity loss of 67 mAh/g. On the other hand, $LiNi_{0.3}Co_{0.3}Mn_{0.3}Fe_{0.1}O_2$ compound in the voltage range 2.8-4.3 V gives an initial discharge capacity of 118 mAh/g with an irreversible capacity loss of 60 mAh/g. The IR drop during the first discharge is about 0.1 V when cycled between 2.8-4.5 V and is about 0.025 V when cycled between 2.8-4.3 V.

To investigate structural changes, we examined the XRD patterns after cycling. The integrated peak intensity ratio of (0 0 3) to (1 0 4) dramatically decreases after cycling. These results show that cation mixing is increased during cycling, especially when cycled in the range 2.8-4.5 V (large amount of Li will be inserted and extracted in this region) compared to 2.8-4.3 V. This result indicates that higher voltage cycling leads to increased cation mixing. Therefore, we found that cation mixing has a very important role in the electrochemical cycling of $LiNi_{0.3}Co_{0.3}Mn_{0.3}Fe_{0.1}O_2$.

ACKNOWLEDGMENT

This work was partially supported by the Assistant Secretary for Energy Efficiency and Renewable Energy, Office of FreedomCAR and Vehicle Technologies of the U.S. Department of Energy under Contract No. DE-AC03-76SF00098.

REFERENCES

1. S.-H. Kang, J. Kim, M. E. Stroll, D. Abraham, Y. K. Sun and K. Amine, *J. Power Sources*, **112**, 41 (2002).
2. H. Arai, S. Okada, Y. Sakurai and J. Yamaki, *Solid State Ionics*, **95**, 275 (1997).
3. T. Ohzuku, A. Ueda and M. Nagayams, *J. Electrochem. Soc.*, **140**, 1862 (1993).
4. T. Ohzuku, A. Ueda and M. Kouguchi, *J. Electrochem. Soc.*, **142**, 4033 (1995).
5. G. Vitins and K. West, *J. Electrochem. Soc.*, **144**, 2587 (1997).
6. Y.-I. Jang, B. Huang, Y.-M. Chaiang and D.R. Sadoway, *Electrochem. Solid-State Lett.*, **1**, 13 (1998).
7. B. Ammundsen and J. Paulsen. *Adv. Mater.*, **13**, 943 (2001).
8. R. J. Gummow and M. M. Thackeray, *J. Electrochem. Soc.*, **141**, 1178 (1994).
9. Y. Makimura and T. Ohzuku, *J. Power Sources*, **119-121**, 156 (2003).
10. N. Yabuuchi and T. Ohzuku, *J. Power Sources*, **119-121**, 171 (2003).
11. T. Ohzuku and Y. Makimura, *Chem. Lett.*, 642 (2001).
12. N. Yabuuchi and T. Ohzuku, *J. Power Sources*, **119-121**, 171 (2003).
13. Y. S. Meng, Y. W. Wu, B. J. Hwang, Y. Li and G. Ceder, *J. Electrochem. Soc.*, **151**, A1134 (2004).
14. C. Wolverton and A. Zunger, *J. Electrochem. Soc.*, **145**, 2424 (1998).
15. A. Rougier, P. Gravereau and C. Delmas, *J. Electrochem. Soc.*, **143**, 1168 (1996).
16. J. Baker, R. Koksbang and M. Y. Saidi, *Solid State Ionics*, **89**, 25 (1996).
17. J.-M. Kim and H.-T. Chung, *Electrochem. Acta*, **49**, 937 (2004).
18. G. T. K. Fey, J. G. Chen, V. Subramanian and T. Osaka, *J. Power Sources*, **384**, 112 (2002).
19. T. Ohzuku and Y. Makihara, *Chem. Lett.*, 642 (2001).
20. S. H. Na, H. S. Kim and S. I. Moon, *Solid State. Ionics.*, **176**, 313 (2005).